Pair-production positron energy-angle distributions of $5m_ec^2$ and $10m_ec^2$ photons on atoms

H. K. Tseng
Department of Physics, National Central University, Chung-Li, Taiwan 32054, Republic of China
(Received 20 March 1995)

With a relativistic partial-wave method we calculated numerically the positron energy-angle distributions of pair production in the field of atoms with atomic numbers $Z=1$ and 92 for photons of energies $k=5m_ec^2$ and $10m_ec^2$. We have found that in this intermediate-photon-energy region, the Born approximation works fine for low-Z elements, as expected. Our partial-wave results indicate that the Born approximation prediction for the shape of positron energy-angle distributions (especially at small positron angles) is better than its prediction for positron energy spectra of pair production in this intermediate-photon-energy region. Our results also show that the shape of positron energy-angle distributions is almost independent of atomic electron screening.

PACS number(s): 32.80.Cy, 32.90.+a

I. INTRODUCTION

Recently it has become feasible to make fairly accurate theoretical calculations of the positron energy spectra of pair production for intermediate-energy photons in the field of atoms [1–3]. In this paper we wish to report predictions for the shapes of pair-production cross sections differential in positron energy and positron angle, to supplement our previous work on the positron energy and positron angle, to supplement our previous work on the positron energy spectra of pair production for photons of energies $k=5$ and 10 [2]. The status of theory and experiment has been summarized by Motz, Olsen, and Koch [3] in their review article on this process. In this work, our results are obtained with a direct numerical calculation by using an exact relativistic partial-wave formulation [2,4]. We describe our basic process as a single-photon production of electron-positron pairs from an unpolarized isolated atom. In addition, we use a simplified model which is adequate for a wide range of atoms and the process at the kinetic energy of the created electron (or positron) above the keV range [5]. The target atom is described by a central potential [5], such as the Hartree-Fock-Slater potential with the exchange term omitted [6].

In Sec. II, we give a brief survey of pair-production theory. In Sec. III, we give and analyze our results for the shape function S of pair-production cross section differential in positron energy E_+ and positron angle θ_+, using the results obtained from the partial-wave method. This shape function is defined as the ratio of the unpolarized pair-production positron energy-angle cross section

$$\sigma(E_+,\theta_+)=[Z^{-2}d\sigma/dE_+d\Omega_+]_{\text{unpol}}$$

to the unpolarized pair-production positron energy spectrum $\sigma(E_+)=[Z^{-2}d\sigma/dE_+]_{\text{unpol}}$.

II. THEORY

Following our previous works [2], we write the pair-production cross section, differential with respect to positron energy E_+ and to positron and electron angles as

$$d\sigma/dE_+d\Omega_+d\Omega_-=(2\pi)^{-5}p_-E_-p_+E_+|M_{fi}|^2 . \quad (1)$$

Here the pair-production matrix element is

$$M_{fi}=(2\pi\alpha/k)^{1/2}\int d^3x\,\psi_2^\dagger(\vec{p}_-,\vec{r},\vec{\zeta}_-)\vec{\alpha}\cdot\vec{\epsilon} \times\psi_1(-\vec{p}_+,\vec{r},\vec{\zeta}')e^{i\vec{k}\cdot\vec{r}} . \quad (2)$$

The photons are specified by momentum $\vec{k}$, energy k, and photon polarization vector $\vec{\epsilon}$ such that

$$\vec{\epsilon}^*\cdot\vec{\epsilon}=1,\quad \vec{\epsilon}\cdot\vec{k}=0 . \quad (3)$$

Here $\psi_2(\vec{p}_-,\vec{r},\vec{\zeta}_-)$ is the electron wave function asymptotically normalized to a unit-amplitude plane wave (or distorted plane wave in the point-Coulomb case) of four-momentum $(E_-,\vec{p}_-)$ and four-polarization $(0,\vec{\zeta}_-)$ in its rest frame plus an incoming spherical wave; and the positron wave function contains asymptotically spherical incoming waves, as the substitutions $E_1\rightarrow -E_+$, $\vec{p}_1\rightarrow -\vec{p}_+$ (but $|\vec{p}_1|\rightarrow|\vec{p}_+|$), and $\vec{\zeta}_1\rightarrow\vec{\zeta}'=\vec{\zeta}_+ -2\hat{p}_+(\hat{p}_+\cdot\vec{\zeta}_+)$ change outgoing into incoming spherical waves, namely,

$$i\gamma^2\psi_+^{\text{in}*}(\vec{p}_+,\vec{r},\vec{\zeta}_+)=\psi_1^{\text{out}}(-\vec{p}_+,\vec{r},\vec{\zeta}') , \quad (4)$$

where ψ_+ is the positron wave function. Using the partial-wave method we used in our previous works [2], we obtain the unpolarized pair-production cross section, differential with respect to positron energy E_+, and to positron angle θ_+,

$$\sigma(E_+,\theta_+)=[Z^{-2}d\sigma/dE_+d\Omega_+]_{\text{unpol}}$$
$$=\lambda_0\sum_{\kappa_2,m=|m_2|}\left[\left|\sum_{\kappa_1}(-1)^{l_1}e^{i\delta_{\kappa_1}}A_+^+\right|^2+\left|\sum_{\kappa_1}(-1)^{l_1}e^{i\delta_{\kappa_1}}A_-^+\right|^2\right.$$
$$\left.+\left|\sum_{\kappa_1}(-1)^{l_1}e^{i\delta_{\kappa_1}}A_+^-\right|^2+\left|\sum_{\kappa_1}(-1)^{l_1}e^{i\delta_{\kappa_1}}A_-^-\right|^2\right], \tag{5}$$

where

$$\lambda_0=\frac{32\alpha}{Z^2k}p_-E_-p_+E_+ , \tag{6}$$

$$A_\pm^+(m)=C_{\kappa_1,m-1}^{\pm}Y_{l_1,m-1\mp1/2}(-\hat{p}_+)R_{\kappa_2\kappa_1}^+(m) ,$$
$$A_\pm^-(m)=C_{\kappa_1,m+1}^{\pm}Y_{l_1,m+1\mp1/2}(-\hat{p}_+)R_{\kappa_2\kappa_1}^-(m) ; \tag{7}$$

$$R_{\kappa_2\kappa_1}^{\pm}(m)=\sum_{n=1}^{2}Q_n^{\pm}(m)\sum_l{}'P_n^{\pm}(m)s_n , \tag{8}$$

and δ_{κ_1} is the positron phase shift for the partial wave κ_1. Here we chose a coordinate system centered at the atomic nucleus with the z axis along $\vec{k}$, $\hat{y}$ along $\vec{k}\times\vec{p}_+$, and $\hat{x}$ in the $(\vec{k},\vec{p}_+)$ plane. In Eqs. (8) the index l runs from $|l_2'-l_1|$ to $(l_2'+l_1)$ in steps of 2 for $n=1$, and from $|l_2-l_1'|$ to (l_2+l_1') in steps of 2 for $n=2$. Here

$$l'=l+\eta_\kappa,\quad \eta_\kappa=-\kappa/|\kappa| ; \tag{9}$$

$$Q_1^{\pm}(m)=\eta_{\kappa_2}(-1)^{m\mp1/2}[(2l_2'+1)(2l_1+1)]^{1/2}$$
$$\times C_{-\kappa_2,m}^{\pm}C_{\kappa_1,m\mp1}^{\mp} ,$$
$$Q_2^{\pm}(m)=-\eta_{\kappa_1}(-1)^{m\mp1/2}[(2l_2+1)(2l_1'+1)]^{1/2} \tag{10}$$
$$\times C_{\kappa_2,m}^{\pm}C_{-\kappa_1,m\mp1}^{\mp} ;$$

$$P_1^{\pm}(m)=(-1)^{(l_2'+l_1-l)/2}T(l_2',l_1,l;m\mp\tfrac{1}{2}) ,$$
$$P_2^{\pm}(m)=(-1)^{(l_2+l_1'-l)/2}T(l_2,l_1',l;m\mp\tfrac{1}{2}) , \tag{11}$$

$$T(l_2,l_1,l;m)=(2l+1)\begin{bmatrix}l_2 & l_1 & l\\ 0 & 0 & 0\end{bmatrix}\begin{bmatrix}l_2 & l_1 & l\\ -m & m & 0\end{bmatrix}, \tag{12}$$

$$C_{\kappa,m}^{\pm}=C(l\tfrac{1}{2}j;m\mp\tfrac{1}{2},\pm\tfrac{1}{2}) ; \tag{13}$$

and

$$s_1=\int_0^\infty dr\, j_l(kr)g_{\kappa_1}f_{\kappa_2} ,$$
$$s_2=\int_0^\infty dr\, j_l(kr)g_{\kappa_2}f_{\kappa_1} . \tag{14}$$

In Eqs. (14) the radial wave functions g_κ and f_κ satisfy the radial Dirac equations

$$dg_\kappa(r)/dr=(p_0+1-V)f_\kappa(r)-\kappa g_\kappa(r)/r ,$$
$$df_\kappa(r)/dr=-(p_0-1-V)g_\kappa(r)+\kappa f_\kappa(r)/r , \tag{15}$$

with $p_0=-E_+$ for ψ_1 and $p_0=E_-$ for ψ_2, where V is the central potential described by the target atom. Also, we obtain the unpolarized pair-production positron energy spectrum

$$\sigma(E_+)\equiv[Z^{-2}d\sigma/dE_+]_{\text{unpol}}$$
$$=\lambda_0\sum_{\kappa_2,\kappa_1,m=|m_2|}\{[R_{\kappa_2\kappa_1}^+(m)]^2+[R_{\kappa_2\kappa_1}^-(m)]^2\} . \tag{16}$$

The problem of calculating the unpolarized pair-production cross sections $\sigma(E_+)$ and $\sigma(E_+,\theta_+)$ has been reduced to computing $R_{\kappa_2\kappa_1}^{\pm}(m)$. We used the similar numerical method we used for our relativistic bremsstrahlung calculations [4]. The $Q_n^{\pm}(m)$ and $P_n^{\pm}(m)$ factors present no great problem. Electron and positron wave functions are obtained in partial-wave series by numerically solving the radial Dirac equation. The radial integrals s_n are calculated numerically to the point where the continuum wave functions of electrons and positrons can be approximately considered as the modified phase-shifted free-field wave functions and an integration by parts method can be used. Then the rest of the radial integrals were calculated by the integration by parts method analytically.

III. RESULTS AND DISCUSSION

With the partial-wave method using Eqs. (5) and (16) we have obtained the shape function of pair production $S=\sigma(E_+,\theta_+)/\sigma(E_+)$ for incident photons of energies $k=5$ and 10, for the elements of atomic number $Z=1$ and 92. These calculated results are shown in Figs. 1–4. In Figs. 1 and 2, we show comparisons of the shape functions S calculated by the numerical partial-wave method (solid lines) with the results calculated by the Born approximation (the crosses) [7], for the cases with $Z=1$ and 92, $k=5$ and 10, and the point-Coulomb potential. The comparison of pair-production positron energy spectrum $\sigma(E_+)$ for these cases is given in Table I. We see that for the cases with $Z=1$ our partial-wave results agree very well with the Born-approximation prediction, as expected. For the cases presented in Fig. 1, the corresponding Coulomb parameters $2\pi Z\alpha E_\pm/p_\pm$ are less than 0.072 and thus the Born approximation is expected to be good. This provides a check of our numerical calculations. However, for the cases with $Z=92$, as shown in Fig. 2 and Table I, we see that the Born-approximation predictions are not good, also as expected. For these cases, the

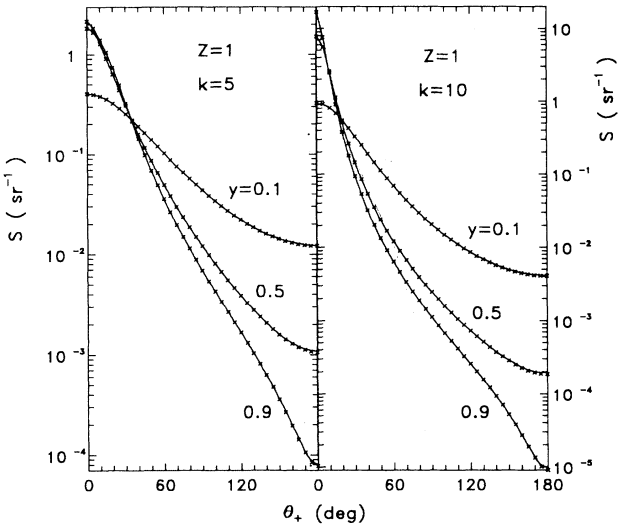

FIG. 1. Comparisons of the shape functions $S=\sigma(E_+,\theta_+)/\sigma(E_+)$ for $Z=1$, $k=5$ and 10, $y=(E_+-1)/(k-2)=0.1,0.5,0.9$, and the point-Coulomb potential between the results obtained by the partial-wave method using Eqs. (5) and (16) (solid lines) and the results obtained by the Born approximation (the crosses).

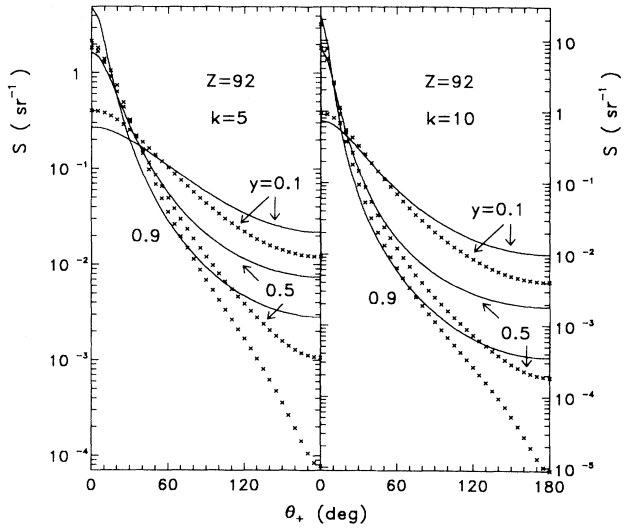

FIG. 2. Same as Fig. 1, except for $Z=92$.

corresponding Coulomb parameters are larger than 4.25. However, our partial-wave results indicate that the Born-approximation prediction for the shape function (especially at small positron angles) is better than its prediction for the positron energy spectrum of pair production in this intermediate-photon-energy region. In Table I, we also show comparisons of unpolarized pair-production cross sections $\sigma_C(E_+)$ by photons of energies $k=5$ and 10 for the case with $Z=92$ between the results of Øverbø, Mork, and Olsen (ØMO) [1] for the point-Coulomb potential and our results calculated with the partial-wave method also for the point-Coulomb potential. The agreement is very good. This provides another check of our numerical calculations.

It is well known [8] that in the high-energy region small positron angles are the main region of the pair-production positron energy-angle cross section $\sigma(E_+,\theta_+)$ which contributes to the pair-production positron energy spectrum $\sigma(E_+)$. From Figs. 1 and 2, we see that as the photon energy k increases, the positron is emitted predominantly at smaller positron angles θ_+, as expected. Under the circumstances that the energies of the created positron and electron $E_\pm \gg 1$, Davies, Bethe, Maximon, and Olsen (DBMO) [8] obtained the high-energy results for the shape function of pair production

$$S_{\mathrm{DBMO}}=\frac{\sigma_{\mathrm{DBMO}}(E_+,\theta_+)}{\sigma_{\mathrm{DBMO}}(E_+)}\ , \tag{17}$$

where

$$\sigma_{\mathrm{DBMO}}(E_+,\theta_+)=\frac{2\alpha^3E_+^2\xi^2}{\pi k^3}\{(E_+^2+E_-^2)(3+2\Gamma)+2E_+E_-(1+4u^2\xi^2\Gamma)\}\ , \tag{18}$$

$$\sigma_{\mathrm{DBMO}}(E_+)=\frac{4\alpha^3}{k^3}\left\{(E_+^2+E_-^2)\left[\int_\delta^1(q-\delta)^2[1-F(q)]^2\frac{dq}{q^3}+1-f(Z)\right]\right.$$

$$\left.+\tfrac{2}{3}E_+E_-\left[\int_\delta^1\left[q^3-6\delta^2q\ln\frac{q}{\delta}+3\delta^2q-4\delta^3\right][1-F(q)]^2\frac{dq}{q^4}+\tfrac{5}{6}-f(Z)\right]\right\}\ . \tag{19}$$

TABLE I. Comparisons of unpolarized pair-production cross sections $\sigma(E_+)$ by photons of energies $k=5$ and 10 in the field of atoms with $Z=1$ and 92 for our results calculated by the partial-wave method for the point-Coulomb potential (σ_C) and for the Hartree-Fock-Slater potential with the exchange term omitted ($\sigma_{\rm HFN}$) with the results of Øverbø, Mork, and Olsen ($\sigma_{\rm \O MO}$) for the point-Coulomb potential, the results calculated with the Born approximation for the point-Coulomb potential ($\sigma_{\rm BH}$), and the results calculated by the high-energy approximation of Davies, Bethe, Maximon, and Olsen ($\sigma_{\rm DBMO}$) for the point-Coulomb potential using Eq. (27). Here $y=(E_+-1)/(k-2)$; $\sigma_{\rm BH}$, $\sigma_{\rm \O MO}$, σ_C, $\sigma_{\rm HFN}$, and $\sigma_{\rm DBMO}$ are in units of $\mu b/m_e c^2$.

Z	k	y	$\sigma_{\rm BH}$	$\sigma_{\rm \O MO}$	σ_C	$\sigma_{\rm HFN}$	$\sigma_{\rm HFN}/\sigma_C$	$\sigma_{\rm DBMO}$
1	5	0.1	91.11		90.82			
		0.5	150.4		150.4			
		0.9	91.11		91.40			
	10	0.1	113.3		113.2			108.4
		0.5	172.5		172.3			171.4
		0.9	113.3		113.4			108.4
92	5	0.1	91.11	36.5	36.53	44.10	1.207	
		0.5	150.4	212.0	212.5	210.4	0.990	
		0.9	91.11	190.0	190.3	184.1	0.967	
	10	0.1	113.3	84.0	83.61	85.06	1.017	34.91
		0.5	172.5	167.0	167.0	162.9	0.975	110.4
		0.9	113.3	148.0	148.1	144.6	0.976	34.91

Here $F(q)$ is the atomic form factor,

$$\delta=\frac{k}{2E_+E_-}\ , \tag{20}$$

$$f(Z)=\sum_{n=1}^{\infty}\frac{(Z\alpha)^2}{n(n^2+Z^2\alpha^2)}\ , \tag{21}$$

$$\xi=\frac{1}{1+u^2}\ , \tag{22}$$

$$u=p_+\theta_+\ , \tag{23}$$

and

$$\Gamma=\ln\frac{1}{\delta}-2-f(Z)+\int_{\delta/\xi}^{\infty}\{[1-F(q)]^2-1\}[q^2-(\delta/\xi)^2]\frac{dq}{q^3}\ . \tag{24}$$

For the point-Coulomb case, the Γ in Eq. (18) becomes

$$\Gamma=\ln\frac{1}{\delta}-2-f(Z)\ , \tag{25}$$

and in Eq. (19) the atomic form factor $F(q)=0$. Then from Eq. (19) we obtain

$$\sigma_{\rm DBMO}(E_+)=\frac{4\alpha^3}{k^3}\left\{(E_+^2+E_-^2)\left[\ln\frac{1}{\delta}-\tfrac{1}{2}-f(Z)+2\delta-\frac{\delta^2}{2}\right]+\tfrac{2}{3}E_+E_-\left[\ln\frac{1}{\delta}-\tfrac{1}{2}-f(Z)+3\delta^2\ln\frac{1}{\delta}+\tfrac{4}{3}\delta^3\right]\right\}. \tag{26}$$

In the high-energy limit, $\delta=k/2E_+E_-$ is very small, and from Eq. (26) we obtain [8]

$$\sigma_{\rm DBMO}(E_+)=\frac{4\alpha^3}{k^3}\{E_+^2+E_-^2+\tfrac{2}{3}E_+E_-\}\times\left\{\ln\frac{1}{\delta}-\tfrac{1}{2}-f(Z)\right\}. \tag{27}$$

Note that when the Coulomb-correction function $f(Z)=0$, Eq. (27) gives the result of the high-energy-limit Born approximation. In Fig. 3, we show comparisons of the shape function S for $Z=1$ and 92, $k=10$, $y=(E_+-1)/(k-2)=0.5$, and the point-Coulomb potential with the results obtained by the partial-wave method (solid lines) and with the results calculated by the high-energy approximation of Davies, Bethe, Maximon, and Olsen (dashed lines) using Eqs. (17), (18), (25), and (27) and the results of the Born approximation (the crosses). For the case with $Z=1$, both the high-energy-approximation and the Born-approximation predictions

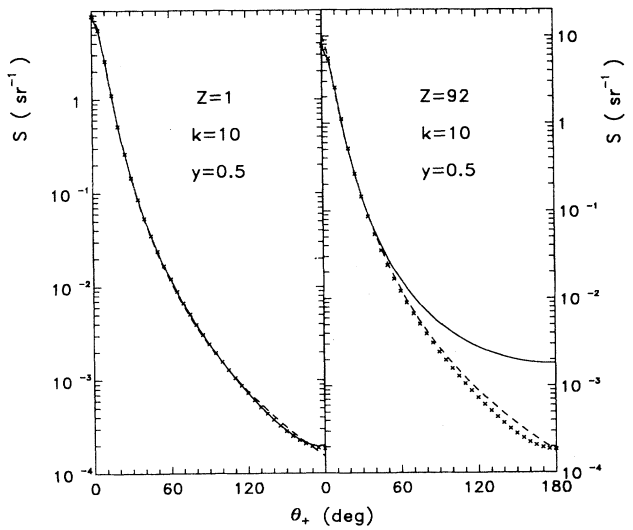

FIG. 3. Comparison of the shape functions $S=\sigma(E_+,\theta_+)/\sigma(E_+)$ for $Z=1$ and 92, $k=10$, $y=(E_+-1)/(k-2)=0.5$, and the point-Coulomb potential for our results calculated by the partial-wave method (solid lines) with the results calculated by the high-energy approximation of Davies, Bethe, Maximon and Olsen (dashed lines) using Eqs. (17), (18), (25), and (27) and the results calculated by the Born approximation (the crosses).

agree well with our partial-wave results for almost all positron angles, while for the case with $Z=92$, the agreement is good only for small positron angles. In Table I, we show the corresponding results of the unpolarized pair-production positron energy spectrum $\sigma_{\mathrm{DBMO}}(E_+)$ calculated with the high-energy approximation for the point-Coulomb potential using Eq. (27). From Table I, we see that the high-energy approximation is poor for the prediction of the positron energy spectrum. This indicates that the energy is not yet high enough for the cases we considered. Note that for the case with $Z=1$ the Coulomb-correction function $f(Z)=6.40\times10^{-5}$ is very small. Thus the difference between the results $\sigma_{\mathrm{DBMO}}(E_+)$ and $\sigma_C(E_+)$ for the case with $Z=1$ comes mainly from the difference between the result of the high-energy-limit Born approximation and the result σ_{BH} [9]. For the case with $Z=92$, the Coulomb-correction function $f(Z)=0.395$, i.e., the Coulomb effect is quite important.

In Fig. 4, we show comparisons of the shape function S for $Z=92$, $k=5$ and 10, $y=(E_+-1)/(k-2)=0.1$, 0.5,0.9 between the results (the solid triangles) obtained by the partial-wave method for the point-Coulomb potential and the partial-wave results (solid lines) for the Hartree-Fock-Slater potential with the exchange term omitted. In Table I, we show the corresponding comparisons of unpolarized pair-production cross section $\sigma(E_+)$. Our results show that the atomic-electron screening effect decreases the cross section $\sigma(E_+)$ for the main region of the positron energy spectra which contributes to the total pair-production cross section, and the effect can be as large as about 21% for the region of low positron energies which contributes little to the total pair-production cross section. Note that the screening increases the cross section $\sigma(E_+)$ for low positron energies. This is because the atomic electrons decrease the Coulomb repulsion of the positrons (which is responsible for the asymmetric positron energy distribution) [10]. For the shape of positron energy-angle distributions, we find that it is almost independent of the screening.

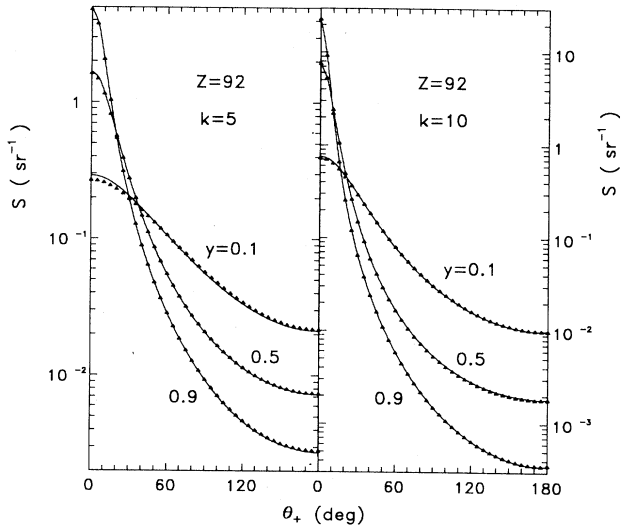

FIG. 4. Comparisons of the shape functions $S=\sigma(E_+,\theta_+)/\sigma(E_+)$ for $Z=92$, $k=5$ and 10, and $y=(E_+-1)/(k-2)=0.1,0.5,0.9$, for the results obtained by the partial-wave method for the point-Coulomb potential (the solid triangles) and the partial-wave results for the Hartree-Slater potential with the exchange term omitted (solid lines).

ACKNOWLEDGMENTS

This work was supported in part by the National Science Council, Republic of China, under Grants No. NSC 83-0208-M-008-026 and No. NSC 84-2112-M-008-001.

[1] L. E. Wright, K. K. Sud, and D. W. Kosik, Phys. Rev. C **36**, 562 (1987); E. Borie, Z. Phys. A **302**, 219 (1981); I. Øverbø, Phys. Lett. **71B**, 412 (1977); I. Øverbø, K. J. Mork, and H. A. Olsen, Phys. Rev. **175**, 1978 (1968); Phys. Rev. A **8**, 668 (1973); I. Øverbø, Ph.D. thesis, University of Trondheim, 1970.

[2] H. K. Tseng, Phys. Rev. A **42**, 6670 (1990); **50**, 343 (1994). Unrationalized units are used throughout, i.e., $\hbar=m_e=c=1$, unless otherwise specified.

[3] J. W. Motz, H. A. Olsen, and H. W. Koch, Rev. Mod. Phys. **41**, 581 (1969).

[4] H. K. Tseng and R. H. Pratt, Phys. Rev. A **3**, 100 (1971).

[5] R. H. Pratt, in *Fundamental Processes in Energetic Atomic Collisions,* edited by H. O. Lutz, J. S. Briggs, and H. Kleinpoppen (Plenum, New York, 1983), p. 145.

[6] D. A. Liberman, D. T. Cromer, and J. T. Waber, Comput. Phys. Commun. **2**, 107 (1971).

[7] R. L. Gluckstern and M. H. Hull, Jr., Phys. Rev. **90**, 1030 (1953); H. A. Bethe and W. Heitler, Proc. R. Soc. London Ser. A **146**, 83 (1934).

[8] H. A. Bethe and L. C. Maximon, Phys. Rev. **93**, 768 (1954); H. Davies, H. A. Bethe, and L. C. Maximon, *ibid.* **93**, 788 (1954); H. A. Olsen, *ibid.* **99**, 1335 (1955); H. A. Olsen and L. C. Maximon, *ibid.* **114**, 887 (1959).

[9] Note that if we use Eq. (26) instead Eq. (27) then the difference between the result of the high-energy-limit Born approximation and the result σ_{BH} will be large.

[10] H. K. Tseng and R. H. Pratt, Phys. Rev. A **4**, 1835 (1971); **6**, 2049 (1972); **21**, 454 (1980); **24**, 1127 (1981). Unfortunately, there are no experimental results available for unpolarized pair-production cross sections $\sigma(E_+)$ and $\sigma(E_+,\theta_+)$ to make comparisons with our calculated results.